p-Methoxy Azobenzene Terpolymer as a Promising Energy Storage Liquid Crystal System

A. Ramadan Ibrahim[†], M. Faisal Khyasudeen[‡], John Husband[†], Sakinah Mohd Alauddin[‡,§], Nurul Fadhilah Kamalul Aripin[‡,§], Thamil Selvi Velayutham[‡,||], Alfonso Martinez-Felipe[¥,£], and Osama K. Abou-Zied*[†]

† Department of Chemistry, College of Science, Sultan Qaboos University, P.O. Box 36, Postal Code 123, Muscat, Sultanate of Oman

‡ Centre for Fundamental and Frontier Sciences in Nanostructure Self-Assembly, Department of Chemistry, Faculty of Science, University of Malaya, 50603, Kuala Lumpur, Malaysia

§ Faculty of Chemical Engineering, Universiti Teknologi MARA, 40450 Shah Alam, Selangor Darul Ehsan, Malaysia

|| Low Dimensional Material Research Center, Department of Physics, Faculty of Science, University of Malaya, 50603 Kuala Lumpur, Malaysia

¥ Chemical and Materials Engineering Research Group, School of Engineering, University of Aberdeen, King's College, Old Aberdeen AB24 3UE, UK

£ Centre for Energy Transition, University of Aberdeen, King's College, Old Aberdeen AB24 3UE, UK

* Corresponding Author: abouzied@squ.edu.om (OKA-Z)

KEYWORDS. side-chain liquid crystal polymers, azobenzene, energy storage, absorption spectroscopy, density functional theory, ultrafast dynamics, dielectric response.

ABSTRACT: Light-responsive materials capable of undergoing photo-induced molecular transformation are excellent candidates for energy storage. Herein we report a promising new liquid crystalline terpolymer that is capable of trapping the absorbed photon energy upon exposure to UV light through *trans* → *cis* isomerization and molecular aggregation. MeOAzB-T (contains *p*-methoxyazobenzene, 2-acrylamido-2-methyl-1-propanesulfonic acid, and methyl(methacrylate) monomeric units) shows a *trans* ← *cis* normal thermal recovery in solution (THF) after UV exposure, whereas in the glassy state (at 22 °C) and smectic phase (at 75 °C) the recovery process indicates an unusual increase in absorbance of the *trans* isomer. Surprisingly, when the smectic phase was cooled down to the glassy state while keeping UV exposure, the increase in absorbance of the *trans* isomer was maintained at the same level in the dark (monitored for 20 days) untill the sample was heated to 75 °C, then cooled to 22 °C in which a full recovery was achieved. Enhancement of H- and J-aggregations of the *trans*-MeOAzB units was found to be responsible for the absorbance increase. Both forms of aggregation have absorbance signatures and were reproduced by time-dependent density functional theory (TD-DFT). A long lifetime component was detected in the femtosecond transient absorption spectra in thin film (215 ps in the glass state and 97 ps in the smectic phase) and was assigned to a long-lived intermediate state as a result of aggregation. The stability of the excited state leads to more aggregation as a consequence of the larger dipole moment, compared to ground state, which is manifested in the TD-DFT calculations as an increase in electron density at the central azo bond. The current results suggest that aggregation after UV irradiation can be maintained for a long time at room temperature, and can be relaxed to the original configuration by heating above the glass transition, showing the suitability of MeOAzB-T as a solar-thermal fuel.

INTRODUCTION

Molecular engineering of novel electrolytes with tailored functionalities is expected to play a major role in improving the efficiency of renewable energy technologies, by enhancing energy harvesting, conversion, and storage processes. More specifically, solar energy irradiated in one hour on the earth's surface (at a 174.7 W m^{-2} rate) matches the yearly energy needed in the world and has an almost unlimited potential to cover the power demand worldwide.[1] The quest for innovative light-responsive materials is crucial to open new frontiers to optimize light harvesting technologies, such as photovoltaics, solar thermal collectors, artificial photosynthesis or solar thermal fuels, and to unlocking their potential to achieve net zero targets.

Photochromic molecules, capable of undergoing photo-induced molecular transformations, are excellent candidates for harnessing solar energy. A wide variety of photoswitches have been investigated over the past decades, including spiropyrans/-oxazine, diarylethenes (*via* pericyclic reactions), azobenzenes, dithienylethene, stilbenes *(via E/Z* isomerizations), triarylmethanes, perchlorotoulenes (*via* photo-induced bond cleavages), anils, polycyclic quinones (*via* intramolecular hydrogen-bond transfer) and viologens (*via* electron transfer).[2-6] Among these, azobenzene has been the most used molecular switch since 1937 when Harley discovered its rapid reversible and high quantum yield of photoisomerization between *E* (*trans*) and *Z* (*cis*) conformations (see **Scheme 1**).[7]

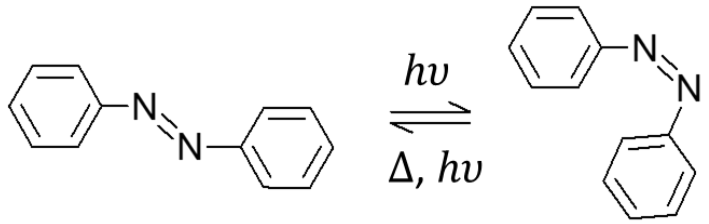

Scheme 1. *Trans*- and *cis*-azobenzene isomers.

By using covalent or supramolecular synthesis, the azobenzene group can be readily attached to other chemical structures, leading to photo-sensitive functional azo-materials. Based on the change of molecular shape promoted by photoisomerization, azo-materials are highly valuable in flexoelectric applications, including micropumps, molecular motors and articulations in robotics.[8, 9] The change in molecular geometry is also very useful in electro-optical devices containing liquid crystalline phases,[10-16] and in biological applications to control the morphology of monolayers, micelles and other assemblies.[17, 18] Pristine azobenzene absorbs UV light at 365 nm, converting solar energy into latent chemical energy, which could then be released through *cis*-to-*trans* isomerization by either thermal relaxation or light irradiation at an appropriate wavelength. More specifically, the storage enthalpy and quantum yield of pristine azobenzene have been calculated to be 49 kJ mol^{-1} and 0.49, respectively, with half-life times of *cis*-azobenzene around 4 days, which are promising for thermal fuels applications.[19-22] The electronic redistribution caused by photon conversion during these processes also makes azobenzene a very promising candidate in photovoltaic applications.

The photochromic properties of new azobenzene derivatives can be tuned by varying the substituents in the aromatic rings, including the light absorption frequency range, quantum yield and the kinetics of back

relaxation to the ground state after irradiation. Recently, we have prepared a series of liquid crystalline poly(methacrylate) random[23-25] and block[26] copolymers containing azobenzene groups at the side chains, which are connected to the polymer backbone *via* flexible alkyl spacers. Liquid crystals (LC) are excellent candidates to integrate and control molecular functions and enhance macroscopic properties, by retaining short-range molecular mobility and long-range order.[27] By introducing polar sulfonic moieties as co-monomers, we have induced conductivity through these azo-polymers, yielding new electrolytes for energy conversion devices. More specifically, we studied the effect of the azobenzene *para*-substitution on the phase and dielectric behavior of terpolymers containing 6-(4-azobenzene−4′-oxy)hexyl methacrylate side-chains (*R*AzB), together with the commercial 2-acrylamido-2-methyl-1-propanesulfonic acid (AMPS), and methacrylate monomers (MMA), see **Scheme 2**.

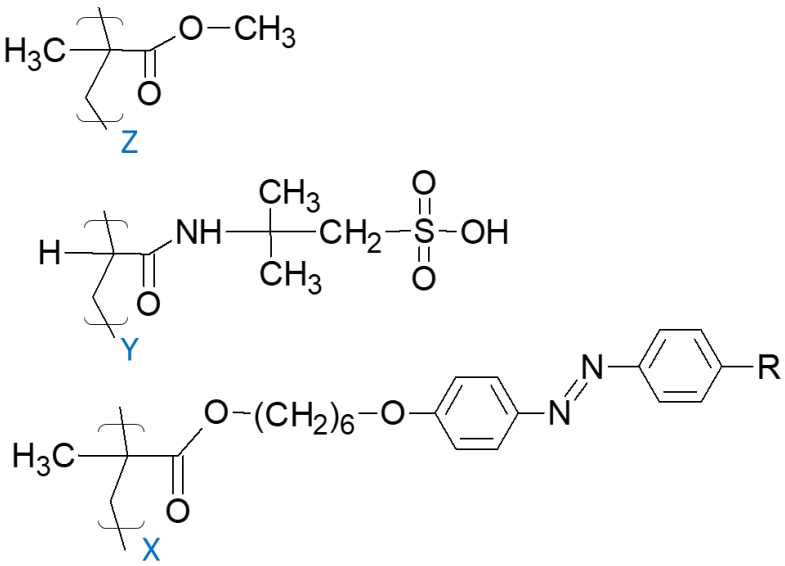

Scheme 2. Chemical structures of the *R*AzB-T terpolymers under study, with different *para*-substitutions on the azobenzene terminal group: methoxy (*R* = MeO), nitro (*R* = NO_2) and non-substituted (*R* = H).

We found that the methoxy-substituted terpolymer, MeOAzB-T, displayed notable conductivity values in the $10^{-2.5}$ S cm^{-1} range,[28] which are among the highest values reported for non-doped liquid crystalline polymers.[29-32] We also observed full recovery of the MeOAzB-T liquid crystalline behavior after irradiation which, together with its high conductivity, makes this terpolymer very attractive for ionic and electronic applications.

In this work, we further explore the potential of MeOAzB-T as a light harvester by studying in detail its spectroscopic response after UV irradiation at different temperatures. In addition, we have carried out theoretical calculations and ultrafast dynamics measurements to unveil the underlying mechanisms for the excitation and relaxation of the azobenzene group in MeOAzB-T. Other polymeric materials presented in **Scheme 2** were also studied in order to explore the unique spectroscopic behavior of MeOAzB-T. Our aim is to correlate the light-response of our materials to their molecular composition, as a way to optimize future light harvesting azo-materials by tuning the electronic effects and local molecular assembly.[33]

EXPERIMENTAL METHODS

Materials Synthesis and Thermal Properties

The synthesis of the three terpolymers under study was carried out by conventional free radical polymerization under an inert atmosphere, which, together with the monomer preparation, was previously described in detail.[28] Briefly, equimolar amounts of the different monomers (the corresponding derivative of 6-(4-azobenzene -4'-oxy)hexyl methacrylate, *R*AzB, the commercial 2-acrylamido-2-methyl-1-propanesulfonic acid, AMPS, and methacrylate, MMA; were added to the reaction vessel and dissolved in polar solvents (e.g., dimethyl formamide)) and were heated to reflux for 24 hours. Reactions were terminated by liquid nitrogen, and the terpolymers were then recovered by precipitation into diethyl ether. The actual molar compositions of the terpolymers were experimentally assessed by ^{1}H-NMR spectroscopy, and their phase behavior by a combination of polarized optical microscopy, POM, and differential scanning calorimetry, DSC.[28] Compositions and thermal parameters are summarized in **Table 1**. The molecular weights of the polymers were obtained by gel permeation/size exclusion chromatography, see **Figure S1**, and the results are summarized in **Table S1**, Supporting Information (SI).

Table 1. Sample names of the RAz-T terpolymers, and experimentally assessed molar percentages of azobenzene (*R*AzB, X), AMPS (Y) and MMA (Z), monomeric units. Glass transitions, T_g, smectic to nematic, T_{SmN}, and nematic to isotropic, T_{NI}, transition temperatures, obtained from the DSC thermograms during their second heating scans.

Sample	**Composition X/Y/Z Molar %**	**T_g / ^{o}C**	**T_{SmN} / ^{o}C**	**T_{NI} / ^{o}C**
MeOAzB-T	40/25/35	74.0	*	135
NO_2AzB-T	21/34/45	97.6	-	-
HAzB-T	21/44/35	73.6	-	-

* Weak transition, merged with T_g.

Among the three terpolymers, only MeOAzB-T shows liquid crystalline behavior, analogous to the MeOAzB homopolymer. More specifically, MeOAzB-T develops smectic phases with d ~ 30.0 Å layer distances, assessed by X-ray diffraction, with the AMPS groups confined between azobenzene layers.[24,34] The smectic template is formed by microphase separation between the polar and non-polar monomers, on cooling from the isotropic melt (T<135^{o}C), and vitrify at temperatures below the glass transition, T_g = 74^{o}C. The formation of a smectic glass can be extremely useful to develop room temperature applications, which is, in part, explored in this work.

Steady-State Absorption and Photoirradiation

UV-visible absorption spectra of 35.9 μM THF solutions and films cast on quartz substrates were measured using an HP 845x Diode Array spectrophotometer. The experiments were carried out at the desired temperatures using a Peltier controller (Quantum Northwest) with a temperature range 0–110 °C and accuracy of ± 0.1 °C. To attain thermal equilibrium, the sample was maintained at the desired temperature for 24 hr before the measurements were conducted. Photoirradiation of the solutions or films was performed using a multiband UV lamp (Mineralight Lamp UVGL-58; 230 V and 6 W) for illumination at 365 nm. The sample was fixed at 10 cm from the lamp with a photon flux of 3.97×10^{14} photon.s^{-1}.cm^{-2} at the sample.

Femtosecond Pump-Probe Transient Absorption

The ultrafast transient absorption measurements were performed using a femtosecond laser setup that was previously described in detail.[35] Briefly, pump and probe pulses were obtained using a regenerative amplified Ti:Sapphire laser (Libra, Coherent). The Libra generates compressed laser pulses (70 fs pulse width) with an output of 4.26 W at a repetition rate of 5 kHz and centered at 800 nm. The output beam was split into two parts. The major portion of the output pulse was used to pump a Coherent OPerA Solo (Light Conversion Ltd.) optical parametric amplifier to generate spectrally tunable light spanning the range 240−2600 nm and is used as the pump beam. The remaining small portion of the laser output was focused on a CaF_2 crystal to generate a white light continuum in the range 330-800 nm, which is used as the probe beam in a Helios transient absorption spectrometer (Ultrafast Systems, LLC). The probe light was measured by a fiber optic coupled to a multichannel spectrometer with a CMOS sensor in the range 350-850 nm. Chirp in the white light continuum probe was minimized by using parabolic mirrors. Rotational contribution to the overall excited state decay kinetics was removed by depolarizing the pump beam using a depolarizer (DPU-25, Thorlabs). The pump pulse was attenuated to ~ 50 nJ in order to avoid multiphoton excitation and photodegradation. The pump and probe pulses were focused on the sample and the temporal delay of the probe pulse was varied using a computer-controlled optical delay stage. Kinetic traces at appropriate wavelengths were assembled from the time-resolved spectral data. Surface Xplorer software (supplied by Ultrafast Systems) was used for data analysis. The instrument-response function (IRF) was measured from Raman scattering to be ~ 100 fs. For solution study, the samples were prepared in 2 mm fused silica cuvettes (Starna Scientific) and were stirred during the experiment. In order to adjust the zero delay for each wavelength and to get the chirp-corrected spectrum, we carried out the transformation process using the software program (Surface Xplore).

Conductivity measurements

The complex permittivity (σ^*) of the samples was determined using a laboratory-built dielectric spectrometer comprised of a function generator, a charge amplifier, and a digital data acquisition system operating at a frequency range of 0.01 to 10^5 Hz. The samples were spin coated on a glass substrate and evaporated with Al electrodes to form a metal-insulator-metal (MIM) structure. The measurements were taken during a step-wise heating process at 5°C intervals between 0 and 165 °C.

RESULTS AND DISCUSSION

Effect of UV Irradiation on Absorption Spectra

Figure 1 shows the absorption spectra of the MeOAzB-T and NO_2AzB-T polymers dissolved in THF before and after irradiation with UV light at 365 nm. Before irradiation, the absorption spectra show a UV peak at 357 nm for MeOAzB-T and 375 nm for NO_2AzB-T. This peak is due to the lowest-energy $\pi^* \leftarrow \pi$ transition in the *trans*-azobenzene chromophore (S_2).[36] The large red shift in the case of the NO_2-substituted polymer can be attributed to the stability of the π^* state as a consequence of migration of the electron density from the donor group (the flexible spacer) to the acceptor group (NO_2) upon electronic excitation. For MeOAzB-T, the two shoulders in the absorption peak were assigned to aggregation of the azobenzene chromophores by stacking the aromatic rings in a head-to-head configuration to form H-aggregates (~ 343 nm) and a head-to-tail configuration to form J-aggregates (~ 373 nm).[17,36] Aggregation in molecules with extended π-conjugation, such as azobenzene, is stabilized by van der Waals interaction and can take place in solution as well as in rigid media. It is clear from **Figure 1** that the presence of an electron-donating group in MeOAzB-T induces aggregation, while the electron-withdrawing group in NO_2AzB-T leads to intramolecular charge transfer that gives rise to more accessible states that produce the observed wide, structureless peak.

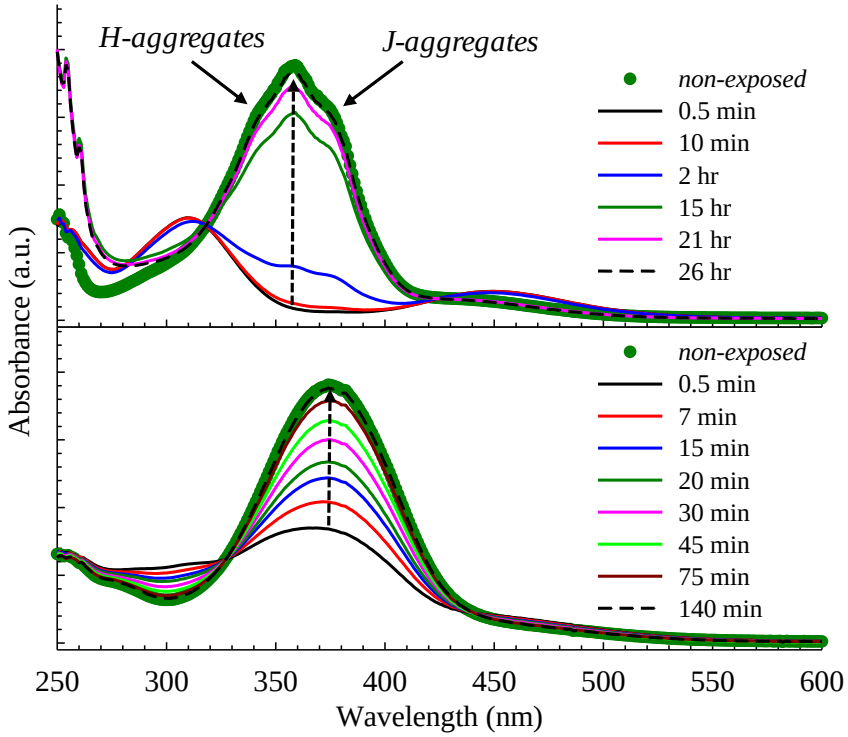

Figure 1. Absorption spectra of MeOAzB-T (upper) and NO_2AzB-T (lower) measured at room temperature for 3.73 x 10^{-5} M THF solutions. Thermal recovery to the original non-exposed samples is shown by dashed arrows after UV irradiation at 365 nm for 10 minutes.

A very small intensity absorption peak in the visible region (420–450 nm) was assigned to a weak $\pi^* \leftarrow n$ transition in *cis*-azobenzene (S_1).[36] This peak is detected in MeOAzB-T, while it is eclipsed by the intense $\pi^* \leftarrow \pi$ absorbance in NO_2Az-T.

Upon irradiation at 365 nm for ten minutes at room temperature, *trans*-to-*cis* isomerization takes place in both polymers. A complete depletion of the *trans* absorbance is clear in MeOAzB-T, with a modest increase in the *cis* absorbance and an emergence of a UV peak at 310 nm. The latter is due to the $S_3 \leftarrow S_0$ transition where the excited S_3 state has a *trans* geometry with a deep minimum at about 90° of twisting.[37] In NO_2AzB-T, the *trans* isomer absorbance decreases by ~ 56% after irradiation and the increase in the absorbance of the *cis* isomer is very small, as well as that of the S_3 state. Thermal *cis*-to-*trans* relaxation in the dark is shown in **Figure 1**. A full recovery of the *trans* isomer takes 26 hr in MeOAzB-T and 140 min in NO_2AzB-T. It is worth noting here that the spectral position of the S_1 state of the *cis* isomer is not sensitive to the nature of substituents in the azobenzene moiety, whereas substitution in the *para*-position by either a donor or acceptor group influences the energy of the π and π^* orbitals and decreases the half-life of the *cis* isomer.[38] This is manifested in the large bathochromic shift of the $\pi^* \leftarrow \pi$ transition in the *trans* isomer of NO_2AzB-T which decreases the energy gap between S_1 and S_2. This point will be discussed in more detail later.

We recently reported the absorption spectra of MeOAzB-T, NO_2AzB-T, and the unsubstituted HAzB-T terpolymers, along with their analogues homopolymers.[28] In film, all polymers show broader $\pi^* \leftarrow \pi$ absorbance than in solution, with the MeO-substituted polymers still maintaining the structured absorbance due to aggregation. In the present work, we studied the *trans* ↔ *cis* isomerization below T_g (glass transition) and in the liquid crystal phase upon UV irradiation, followed by recovery in the dark. The ability of azobenzene to isomerize *via* the inversion mechanism allows this dynamical process to easily take place in rigid matrices as a consequence of the much smaller free volume required during isomerization than in the rotational mechanism.[38,39] The latter involves a large energy barrier and requires large free volumes, making it impossible in glassy polymers.

With the exception of the NO_2AzB-based analogues, all polymers studied here show reversible isomerization in film. We could not observe a clear *trans* → *cis* isomerization in NO_2AzB-T or its homopolymer, which may be due to the electron-withdrawing property of the NO_2 group that induces intramolecular charge transfer from the polymer side. The small energy difference between the S_1 and S_2 states may also induce an appreciable mixing between them, which prevents clear separation between the two isomers upon excitation. These two factors are expected to be more dominant in film than in solution.

Figure 2 displays representative absorption spectra of MeOAzB-T collected at 22 °C (below T_g) and 75 °C (smectic phase) before exposure to UV light, and then during recovery in the dark. A detailed behavior (absorbance change as a function of time) for the recovery process in each case is presented in **Figure 3**. We start first with the results at the glass state. Exposure to UV light induces smaller 365 nm peak reduction than in solution, which we attribute to a lesser extent of *trans*-to-*cis* isomerization caused by the rigid environment in the glass. We estimated the quantum yield of photoisomerization in glass to be 23% (**Table S2** and **Figure S2**, SI). Upon recovery in the dark at 22 °C, the *cis* isomer relaxes back (by thermal activation) following an expected pattern, but takes a very long time for a full recovery (365 hr), once again attributed to steric restrictions. On the other hand, the *trans* isomer shows an initial fast recovery in its absorbance, which, unexpectedly, then continues to increase beyond the non-exposed state. This increase continues for 4 hr before a decrease in the absorbance starts. The final stage of recovery spans a long time (361 hr) before the absorbance intensity is close to that of the non-exposed sample. To our knowledge, this is the first time such behavior is reported for materials containing the azobenzene chromophore.

The unusual increase in the *trans* isomer's absorbance can be correlated to the enhancement of aggregation after irradiation and during the recovery period. This is not surprising since aggregation is possible in

solution as well as in the solid state. More insight into this behavior can be provided by considering the mean-field model that describes the photoinduced surface reliefs in dye containing side-chain polymers.[40] In this model, each chromophore experiences a local potential resulting from the other chromophore dipoles in the material. Upon irradiation, chromophores tend to orient by the effect of the electromagnetic radiation, and this net orientation induces an overall potential that naturally aligns other chromophores in the vicinity. Additionally, the attractive force between chromophores that are aligned similarly leads to a net force on chromophores in the illuminated area, causing them to assemble in aggregates.

We note that this unusual behavior was not observed for the *cis* isomer at 450 nm (aggregation is not possible for the *cis* isomer due to its bent structure, recall Scheme 1). However, recovery of the 450 nm peak takes the same time interval as the *trans* isomer. This may point to mixing of *trans* and *cis* states in the 450 nm region in which full recovery can only be attained when the *trans* isomer returns to the non-exposed level. We will investigate this point in more details in the following sections.

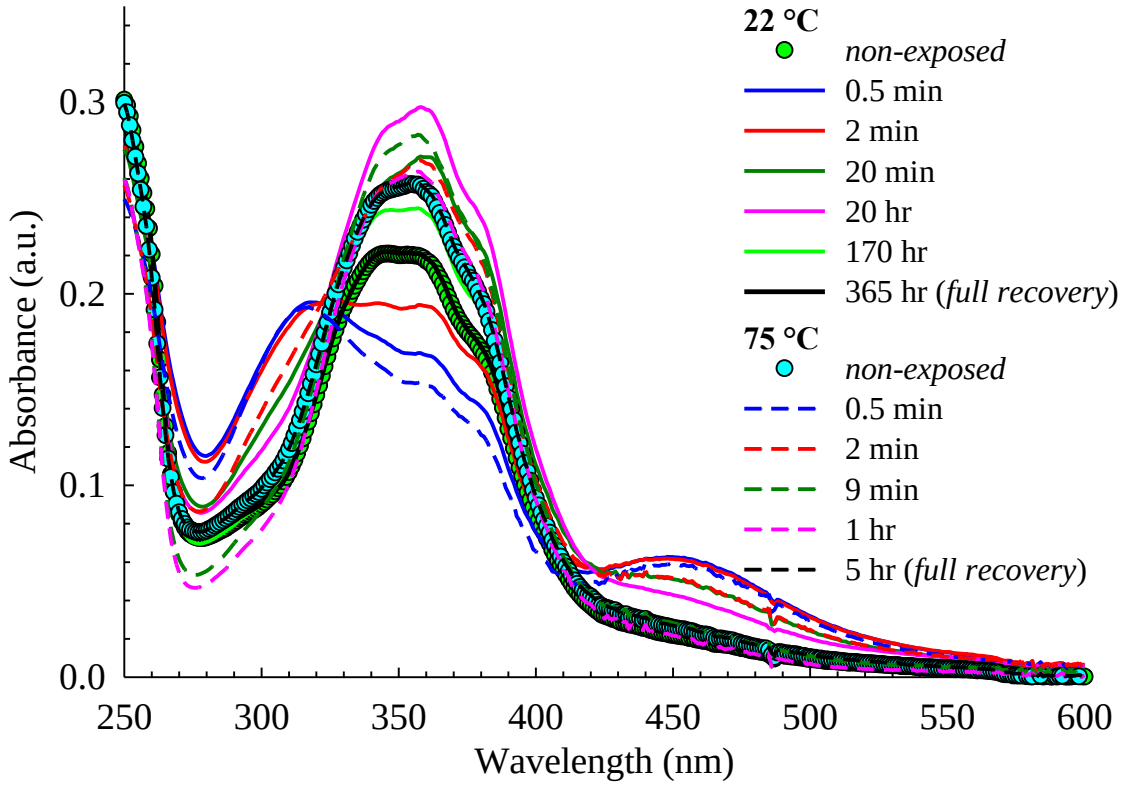

Figure 2. Representative absorption spectra of MeOAzB-T film cast on a quartz substrate at 22 °C (glass state) and 75 °C (smectic phase) before and after UV irradiation at 365 nm for 10 minutes.

Illumination at the smectic phase of MeOAzB-T (heating to 75 °C for 2 hr) results in a slight increase in absorbance (**Figures 2** and **3**). After exposure to UV light, the behavior was similar to that reported above, but with a much faster recovery (5 hr). The slight increase in absorbance indicates the tendency to form more aggregates in the liquid crystalline state and the faster recovery is due to the thermal activation of the groups, taking place at temperatures higher than that of the glass. Similar results in glassy and liquid

crystalline phases were obtained for the homopolymer MeOAzB-H (data not shown), and can be related to the high values of activation energy observed in dielectric relaxations of the azobenzenes.[28]

In order to clarify the correlation between chemical structure, aggregation and UV absorption in MeOAzB-T, we carried out similar experiments on the unsubstituted HAzB-T terpolymer (**Figures S1** and **S2**, Supporting Information (SI)). In this terpolymer, no clear signs of H/J-aggregates were observed for the *trans* isomer and the results show expected recovery to the initial state of the non-exposed samples.

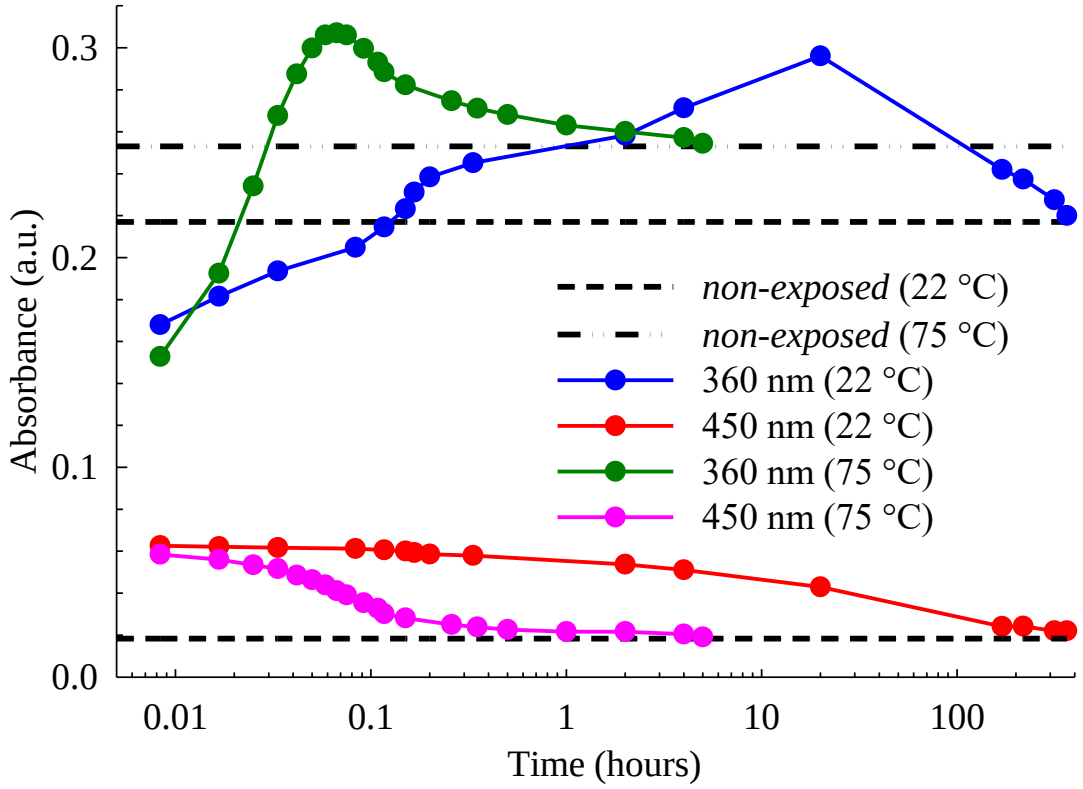

Figure 3. Detailed behavior of absorbance recovery to the original non-exposed level for the *trans* (360 nm) and *cis* (450 nm) isomers of MeOAzB-T film cast on a quartz substrate at 22 °C (glass state) and 75 °C (smectic phase) after UV irradiation at 365 nm for 10 minutes.

Theoretical Modeling

The previous results highlight the importance of chemical composition on the UV response of the terpolymers under study, *via* aggregation and molecular mobility. We have further explored the effect of *para*-substitution at the azobenzene moiety on the electronic distribution of our samples, by using five *para*-substituted model chromophores: NO_2AzBH; MeOAzBH; HAzBOPr; NO_2AzBOPr; and MeOAzBOPr, which have been investigated using density functional theory (DFT) at the CAM-B3LYP/6-31G(d) level as implemented in Gaussian 09[41] (Pr indicates propyl group). Time-dependent (TD-DFT) calculations at the optimized ground-state geometries were used to predict vertical excitation energies to the lowest 100 singlet excited states. For similar azobenzene derivatives, the employed methodology has recently been benchmarked against MS-RASPT2/RASSCF/ANO-LVDZP calculations, and shown to give very good

agreement between the calculated excitation energies and experimental, gas-phase, absorbances (within 0.04 eV and 0.25 eV respectively for the $\pi^* \leftarrow \pi$ and $\pi^* \leftarrow n$ transitions in both *trans*- and *cis*-azobenzene).[42]

Table 2 lists the calculated excitation wavelengths to the first- and second-excited states in the non-substituted *trans*- and *cis*-azobenzene isomers, corresponding to the lowest energy $\pi^* \leftarrow n$ and $\pi^* \leftarrow \pi$ transitions respectively. For the five model chromophores, wavelength-shifts with respect to azobenzene are indicated. For the $\pi^* \leftarrow \pi$ transitions, the predicted shifts correlate well with the electron donating/withdrawing characteristics of the substituents. Considering first the series AzB, NO_2AzBH, MeOAzBH, the addition of either the electron withdrawing nitro group or the donating methoxy group increases the molecular dipole and causes a similar-sized red-shift in the absorbance. This is true for both *cis* and *trans* isomers.

We now study the effect of the terminal chain through the OPr series, where the propoxy group has been added to mimic (to some extent) the six methylene spacer linking the azobenzene group to the backbone in our polymers. HAzBOPr shows the same behavior as MeOAzBH, while the largest red-shifts are predicted for the doubly substituted NO_2AzBOPr and MeOAzBOPr. NO_2AzBOPr is a D-π-A, or push-pull system, in which the paring of electron donating and accepting groups creates a large dipole moment along the molecular axis, and in which the $\pi^* \leftarrow \pi$ transition further increases the dipole in the excited state by transferring charge from the donor side of the molecule to the acceptor side – **Figure 4a**. Conversely, MeOAzBOPr may be considered a D-π-D, push-push system, and the $\pi^* \leftarrow \pi$ transition transfers charge from the exterior of the molecule to the central azo bond – **Figure 4b**. The π^* state is more stabilized in the D-π-A system than in the D-π-D system, resulting in the larger red-shift. The calculated excitation energies for these gas-phase, model chromophores are ~ 40 nm higher than for the corresponding homo- and ter-polymers.[28] However, the predicted order and relative shift in absorbances for the series HAzBOPr, NO_2AzBOPr, MeOAzBOPr match well with the recorded spectra, indicating that, while the azo moiety is electronically isolated from the polymer backbone, the spacer group must be taken into account when considering its electronic properties.

The $\pi^* \leftarrow n$ transitions are symmetry forbidden in the *trans* isomers and only weakly allowed in the *cis* isomers. The position of this band is largely unchanged for the studied *cis* isomers, while for the *trans* isomers a blue shift is associated with electron donating groups and a red shift is calculated for the withdrawing, nitro, group. In push-pull substituted azobenzenes, increased efficiency for *trans-cis* photoisomerization has been linked to a decrease in the S_1–S_2 energy gap that can be tuned by adjusting the strength of the electron accepting/donating group.[43] A reduction in the S_1–S_2 energy gap eases the crossing from S_2 to S_1 following irradiation, and opens the possibility for direct photoexcitation to S_1. Compared to azobenzene, the S_1–S_2 energy gap is 0.45 eV less in NO_2AzBOPr and is also reduced by a similar amount (0.48 eV) in MeOAzBOPr.

Focusing on MeOAzBOPr, as a highly simplified approximation of the proposed aggregates in MeOAzB-T, two units of MeOAzBOPr have been used to mimic H- and J-aggregates. For the H-type aggregate, the two units are superimposed on top of each other with an inter-unit separation of 4.0 Å, while for the J-type, the units are offset to align opposing phenyl rings; the inter-unit separation is again set to 4.0 Å – **Figure 5**. The structures were prepared "by hand" with no attempt to optimize them. Parallel and anti-parallel arrangements with respect to the MeO and PrO groups gave minimal differences in calculated excitation energies for either of the aggregate types. Likewise, inter-unit separations of 3.5 – 4.5 Å gave minimal differences in calculated excitation energies. TD-DFT CAM-B3LYP/6-31G(d) calculations were

performed to predict vertical excitation energies to the lowest 20 singlet excited states at the starting geometry. The resulting output is convoluted with a gaussian function of fwhh 6000 cm^{-1} to yield the simulated spectra shown in **Figure 5**. Despite the simplicity of the models, there is obvious similarity between the relative positions of the intense $\pi^* \leftarrow \pi$ transition in the simulated spectra and the features seen in the MeOAzB-T spectra. The pertinent molecular orbitals involved in the $\pi^* \leftarrow \pi$ transitions are shown in **Figure S4, SI**. For the H-type aggregate the major contributions are LUMO ← HOMO-1 (47%), and LUMO+1 ← HOMO (49%). Each of these orbitals is distributed over both of the molecular units, and the transition can be seen to transfer electron density from the edges of the molecules to the central azo bond as previously discussed for the isolated molecule. For the J-type aggregate the transition is more complex. LUMO ← HOMO-1 and LUMO+1 ← HOMO are again involved, although to a lesser extent (29% and 5% respectively), while the largest contribution (49%) comes from LUMO ← HOMO, with a further minor (5%) contribution from LUMO+1 ← HOMO-1. Interestingly, while the HOMO-1 and HOMO orbitals are evenly distributed over both of the molecular units, the LUMO and LUMO+1 orbitals are each centered on one or other of the monomer units.

Analogous calculations for NO_2AzBOPr (results not shown) give similar simulated spectra, suggesting that the featureless absorption peak seen in the NO_2AzB-T spectra is indicative of minimal aggregation in this system.

In their study of the non-covalent interactions in Langmuir–Blodgett films, Tang *et al*. demonstrated that the density of packing and the strength of the electronic coupling in azobenzene derivatives was dependent on the relative strengths of the intermolecular dipolar and π-π stacking interactions.[44] Higher packing density is favored in systems with low molecular dipoles (MeOAzB-T) while strongly polar molecules (NO2AzB-T) gave rise to much more loosely packed configurations, as we have observed in our UV absorption experiments.

Table 2. TD-DFT CAM-B3LYP/6-31G(d) gas-phase, vertical excitation energies (nm) for azobenzene and energy shifts (nm) relative to azobenzene for the five studied model chromophores. Oscillator strengths are given in parentheses and gas-phase, experimental values for azobenzene in braces.

	Az {exp. [43]}	NO_2AzBH	MeOAzBH	HAzBOPr	NO2AzBOPr	MeOAzBOPr
			trans			
$S_2 \leftarrow S_0$	295 {301}	+13	+15	+19	+40	+28
$[\pi\pi^*]$	(0.80)	(0.96)	(0.94)	(0.95)	(1.10)	(1.10)
$S_1 \leftarrow S_0$	450 {440}	+15	-11	-8	+7	-19
$[n\pi^*]$	(0.00)	(0.00)	(0.00)	(0.00)	(0.00)	(0.00)
			cis			
$S_2 \leftarrow S_0$	259 {265}	+17	+15	+20	+37	+22
$[\pi\pi^*]$	(0.16)	(0.23)	(0.24)	(0.06)	(0.07)	(0.16)
$S_1 \leftarrow S_0$	451 {425}	+4	+2	-2	+1	-1
$[n\pi^*]$	(0.02)	(0.03)	(0.03)	(0.02)	(0.03)	(0.03)

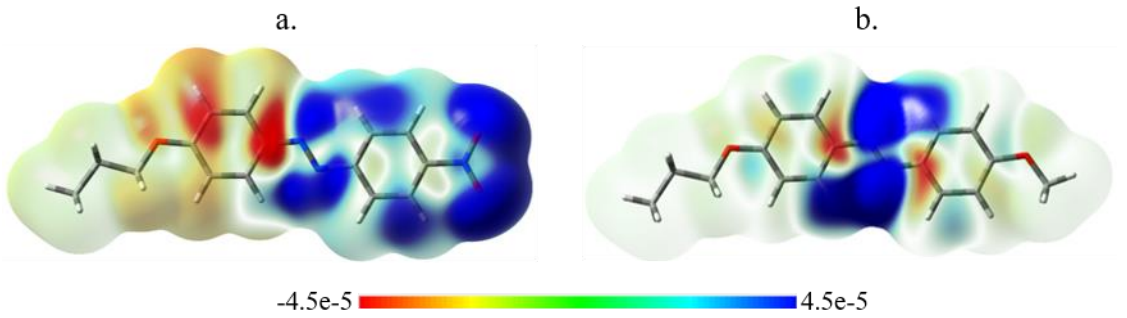

Figure 4. Electron density difference plots for a. *trans*-NO_2AzBOPr and b. *trans*-MeOAzBOPr. The difference in electron density ($S_2 - S_0$) is mapped onto the ground state density at an isosurface of 0.004. Blue shades indicate an increase in electron density in the excited state.

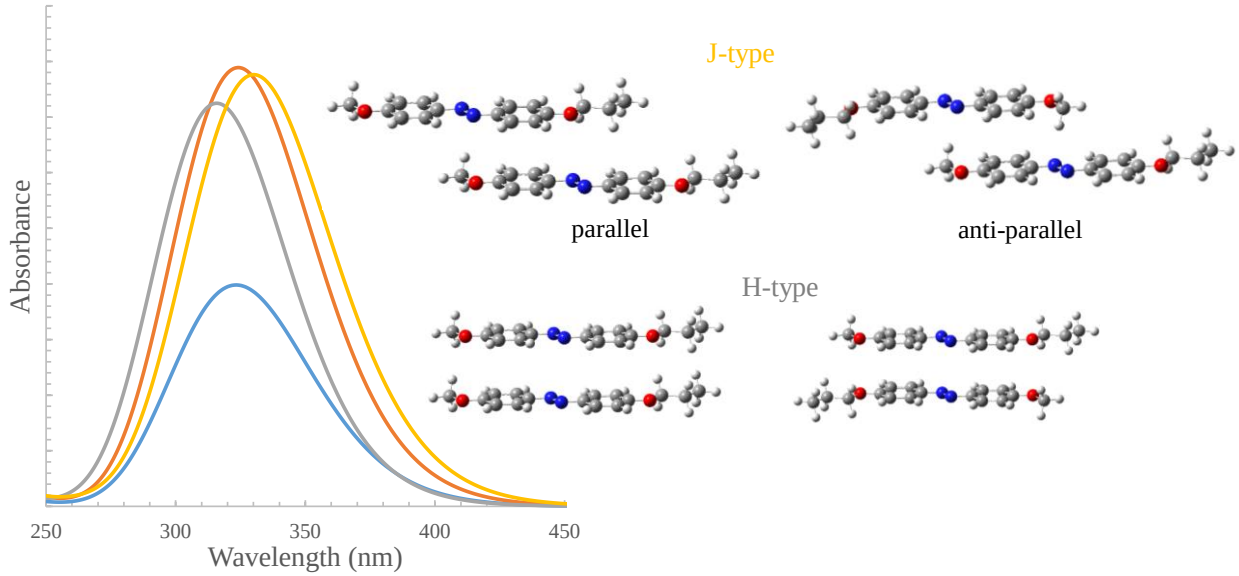

Figure 5. Simulated absorption spectra from TD-DFT CAM-B3LYP/6-31G(d) calculations of model aggregate structures based on two units of MeOAzBOPr. Parallel and anti-parallel arrangements give essentially identical spectra. Included are simulated spectra for a single MeOAzBOPr monomer (blue) and for an H-type aggregate in which the inter-unit distance has been set to 10 Å to mimic a non-interacting pair (red).

Ultrafast Dynamics

To further understand the mechanisms behind the photo-induced response of MeOAzB-T, we performed a series of femtosecond transient absorption (TA) spectroscopic measurements for this polymer, in THF solution, and on one film cast on a quartz substrate measured at 22 °C (glass state) and 75 °C (liquid crystalline smectic phase). **Figure 6** depicts snapshots of the TA spectra at different delay times between the pump pulse (λ_{pump} = 360 nm) and the probe pulse. The spectra show a ground-state bleach (GSB) band

in the 340-380 nm region that is distorted by the excitation pulse, and a broad excited-state absorption (ESA) band that covers the 390-700 nm region. Excitation at 360 nm promotes the ground state *trans* isomer to the S_2 state ($\pi^* \leftarrow \pi$). The GSB band reflects the dynamics of this transition. On the other hand, the ESA band could be due to the *cis* or the *trans* isomer. We observed a similar ESA band after excitation at λ_{pump} = 450 nm, which corresponds to the $\pi^* \leftarrow n$ transition ($S_1 \leftarrow S_0$). The ESA band is thus due to a mixture of *trans* and *cis* isomers. This can be interpreted on the basis of the potential energy surfaces of the azobenzene isomers in which the energy gap between the S_1 and S_2 states determines the reaction pathway.[45,46] This energy gap was reported to be ~ 11,000 cm^{-1} in pristine azobenzene,[44,47] and is reduced by *para*-substitution.[48-50] In the case of MeOAzB-T, we calculated the S_1–S_2 energy gap from **Table 2** to be 7782 cm^{-1} (modeled as MeOAzB-OPr). Based on the overestimation of the observed absorption bands, the S_1–S_2 energy gap in MeOAzB-T is likely to be less. As the energy gap gets smaller, the molecular structure of the azobenzene moiety has more characters of the *trans* form at the crossing between the two states. This proximity between the two states results in the possibility of direct excitation of the *trans* isomer to the S_1 state ($\pi^* \leftarrow n$).[48,49,51] Although this transition is electric-dipole forbidden, it may become allowed by coupling with vibrations that induce nonplanar distortion.[52] This vibronically allowed transition can borrow intensity from the nearby allowed $\pi^* \leftarrow \pi$ electronic transition. The intensity borrowing mechanism is more efficient as the S_1–S_2 energy gap becomes smaller.

The TA spectra for the glass and smectic phases are proportional to the spectral difference between before and after irradiation in the steady-state absorption spectra (shown in the upper segment in **Figure 6**). The reduced resemblance for MeOAzB-T in THF may be due to the much larger effect of UV irradiation which causes a complete bleach of the *trans* absorbance (**Figure 1**). In THF, the ESA band can be seen as two separate broad bands (390-450 nm and 450-700 nm), whereas in thin film the two bands are more diffused.

Quantitative analysis of the TA data was performed by fitting the transients to a multiexponential decay function with amplitudes α_n and decay constants τ_n. It was not possible to perform a reliable fit for the GSB band due to the large scattering from λ_{pump}, but it is clear that this band recovers exponentially by time. We then proceed with analysis of the ESA band. The kinetic traces at λ_{probe} = 400-420 nm are shown in **Figure S5, SI** and the values are summarized in **Table 3**. The first time constant (τ_1 ~ 100 fs) was observed as a buildup time for MeOAzB-T in solution and smectic phase, but was not observed in the glass state. This dynamical process reflects the transfer of the wave packet away from the Franck-Condon region immediately after excitation to the S_2 ($\pi\pi^*$) state by vibrational relaxation and internal conversion to the S_1 ($n\pi^*$) state. The similar magnitude of τ_1 in solution and film implies that the azobenzene molecule remains in the *trans* form during this dynamical process. The second time constant, τ_2, is ascribed to the span of the *trans-cis* isomerization and excited-state relaxation through the conical intersection (S_1/S_0). From our analysis, all the MeOAzB-T samples show τ_2 = 2-3 ps, which concur with the reported values for other azobenzene derivatives in various solvents (1.3-3.5 ps).[53-58] There is a small increase in this time constant in the smectic phase and solid matrix, compared to solution, which may reflect the minor effect of the rigid environment on this dynamical process. This observation points to the mechanism of isomerization that follows the inversion process, rather than the rotational pathway that requires more energy and space. In contrast to the latter, the inversion path to isomerization is barrierless and involves little change in the total volume during isomerization.[38,39] This mechanism of isomerization was confirmed by observing no effect of solvent viscosity on the azobenzene derivative *trans*-4-aminoazobenzene.[51] *Trans* ↔ *cis* isomerization *via* the inversion pathway makes it possible to induce this process efficiently in a solid matrix such as ours, and can be favored by planar arrangements, like those in smectic phases. The absence of τ_1 in the glass may be due to a very small contribution that we could not detect within the signal-to-noise level.

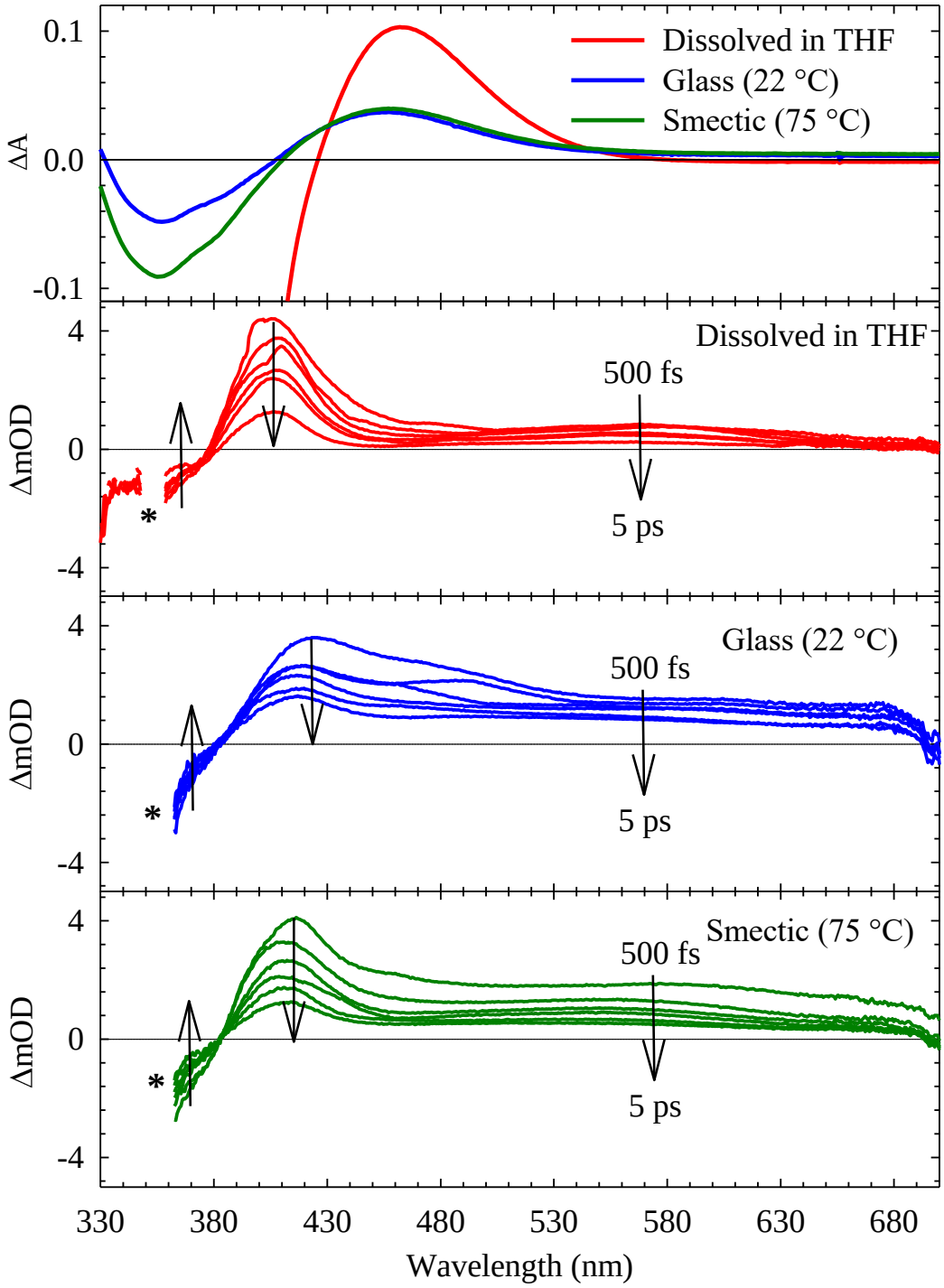

Figure 6. Transient absorption spectra of MeOAzB-T in THF solution, and film cast on a quartz substrate measured at 22 °C (glass state) and 75 °C (smectic phase). The spectra display snapshots at different delay times between the pump pulse (λ_{pump} = 360 nm) and the probe pulse. *: scattered light from λ_{pump}. Upper segment: difference between the steady-state absorption spectra (taken from the spectra in Figures 1 and 2) of the non-exposed samples and right after exposure to UV light.

The third decay component in the transients (τ_3 in **Table 3**) was measured to be 5.4 ps in THF and the value gets much longer in thin film: τ_3 = 62 ps in the glass phase (22 °C), and τ_3 = 27 ps in the smectic phase (75 °C). The considerable sensitivity of this decay component to the local environment may imply a mechanism of isomerization that requires certain critical free volume. A possible scenario for this mechanism is by considering the existence of a "bottleneck" excited state that can only be reached by rotation along the –N=N– reaction coordinate.[59] This rotational mechanism was used to explain the ultrafast measurements on side-chain polymeric azobenzenes where a long component (160 ps) becomes much longer (430 ps) after cross-linking.[60] On the other hand, an alternative assignment for τ_3 of azobenzene derivatives in solution was provided as vibrational cooling in the ground state (5-20 ps).[51,61] In our system, the much longer component in the glassy matrix (τ_3 = 62 ps), compared to liquid crystal (τ_3 = 27 ps), must be due to the rigid, confined glass environment which becomes slightly flexible in the liquid crystalline state. We observed a similar component upon excitation at 450 nm ($n\pi^*$ excitation). This time constant should then correspond to another channel for the *trans* isomer to relax to the ground state from S_1 (a similar observation was reported for azobenzene in acetonitrile).[53]

Table 3. Ultrafast dynamics of MeOAzB-T in THF, glass state, and in liquid crystalline smectic phase. λ_{pump} = 360 nm.

	τ_1, fs (α_1)	τ_2, ps (α_2)	τ_3, ps (α_3)	τ_4, ps (α_4)
λ_{probe} = 400-420 nm				
MeOAzB-T (in THF)	120 ± 24 (-0.42)	2.06 ± 0.64 (0.26)	5.4 ± 0.8 (0.32)	
MeOAzB-T (glass, 22 °C)		3.08 ± 0.33 (0.45)	62 ± 5 (0.57)	
MeOAzB-T (smectic, 75 °C)	96 ± 36 (-0.34)	2.25 ± 0.16 (0.47)	27 ± 4 (0.19)	
λ_{probe} = 550 nm				
MeOAzB-T (in THF)	223 ± 24 (-0.49)	2.23 ± 0.47 (0.33)	7.4 ± 1.6 (0.18)	
MeOAzB-T (glass, 22 °C)		2.96 ± 0.35 (0.35)	24 ± 3 (0.36)	215 ± 35 (0.29)
MeOAzB-T (smectic, 75 °C)	96 ± 36 (-0.55)	1.65 ± 0.20 (0.29)	15 ± 2 (0.08)	97 ± 15 (0.08)

The last detection window was at λ_{probe} = 550 nm in **Figure 6**. The transients are shown in **Figure 7** and the decay constants are included in **Table 3**. No change within the measurements uncertainty was observed for MeOAzB-T in THF, or for the first two components in thin film. On the other hand, τ_3 shows a large drop in its value in the glass (τ_3 = 24 ps) and the smectic phase (τ_3 = 15 ps), compared to the corresponding

values at λ_{probe} = 400-420 nm. An additional much longer time constant was also observed in both phases (τ_4 = 215 ps in glass and τ_4 = 97 ps in smectic phase; see **Figure S6, SI** for comparison between the transients measured at λ_{probe} = 410 nm and λ_{probe} = 550 nm). This observation may indicate the presence of a long-lived intermediate (characterized by τ_4) that interacts with the initially populated state (characterized by τ_3). This long decay component may be assigned to aggregation of the terpolymer which stabilizes the excited state. This, in turn, leads to more aggregation as a consequence of the larger dipole moment, compared to ground state, which is manifested in the increase in electron density at the central azo bond in the excited state (see **Figure 4**). According to the mean-field model discussed earlier, more molecules will tend to align and aggregate as a result of the increased dipoles in the material which is observed in the enhanced absorbance of the *trans* isomer beyond the non-exposed state during the recovery process after exposure to UV light (**Figure 2**).

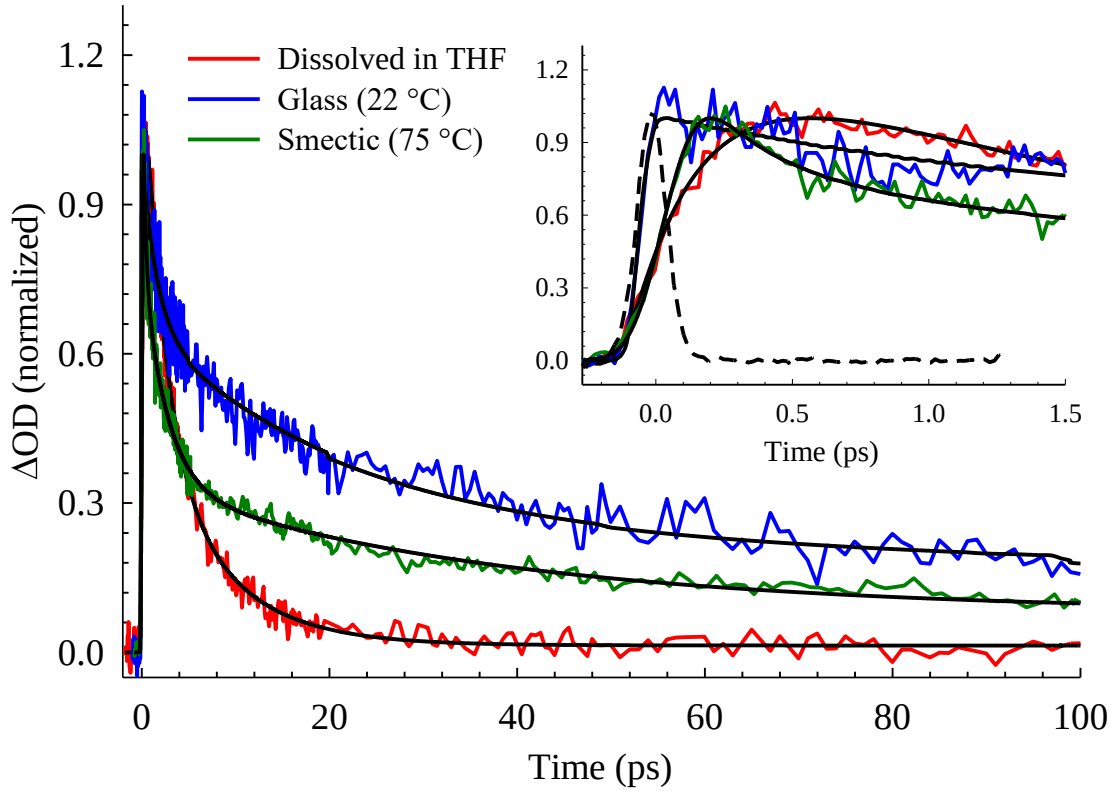

Figure 7. Kinetic traces of MeOAzB-T terpolymer measured in THF solution, and film cast on a quartz substrate at 22 °C (glass state) and 75 °C (smectic phase). Inset shows an expanded time window of 1.5 ps (IRF is shown in dashed line). λ_{pump} = 360 nm and λ_{probe} = 550 nm. Fits to a multiexponential decay function are shown in black solid lines.

Energy Storage Model

The unusual increase in absorbance in the dark after illumination of MeOAzB-T is intriguing and may be promising in applications involving optical and energy storage through long-term stability of the aggregated

trans isomer. With this in mind, we carried out another steady-state illumination experiment on the smectic phase of MeOAzB-T by irradiating UV light at 365 nm for 10 minutes at 75 °C, followed by rapid cooling while keeping the UV illumination on until the sample temperature reached 22 °C (glass state). We then measured the recovery process in the dark, which is plotted in **Figure 8** for the corresponding peaks of the *trans* and *cis* isomers. At 22 °C, and after a slight drop from the maximum intensity, the absorbance maintains its value for up to 480 hr (20 days). We then heated the sample to 75 °C and observed an immediate decrease in absorbance. A full recovery to the absorbance level of the non-exposed liquid crystalline sample was attained after 20 minutes. This level was maintained until we cooled the sample to 22 °C, in which a second decrease in absorbance was observed. A final recovery in absorbance to the initial level of that of the non-exposed glass state was reached within ~ 5 minutes. We performed the same experiments on the HAzB-T sample (**Figure S3**, SI) and the results show a continuous recovery of the absorbance at 350 nm until a full recovery was reached after 96 hr, confirming the role of molecular aggregation in trapping the energy in MeOAzB-T.

These findings imply that the new aggregate state can be maintained at room temperature for an extended period of time and can be further unlocked by heating above its glass transition temperature. Additionally, the polar sulfonic groups impart a significant conductivity response to MeOAzB-T (with a dc conductivity of σ_{dc}~$10^{-3.5}\ Scm^{-1}$ and a dielectric constant in the range of $10 < \varepsilon' < 10^3$; see **Figure S7, SI**).[28] As a result, we believe that this material possesses considerable potential as an organic nano-electrolyte. The recovery to the smectic phase initial state (i.e. heating to 75 °C) could be used to release energy via a variety of external stimuli that promote molecular mobility, including thermal, mechanical, or chemical stimuli.

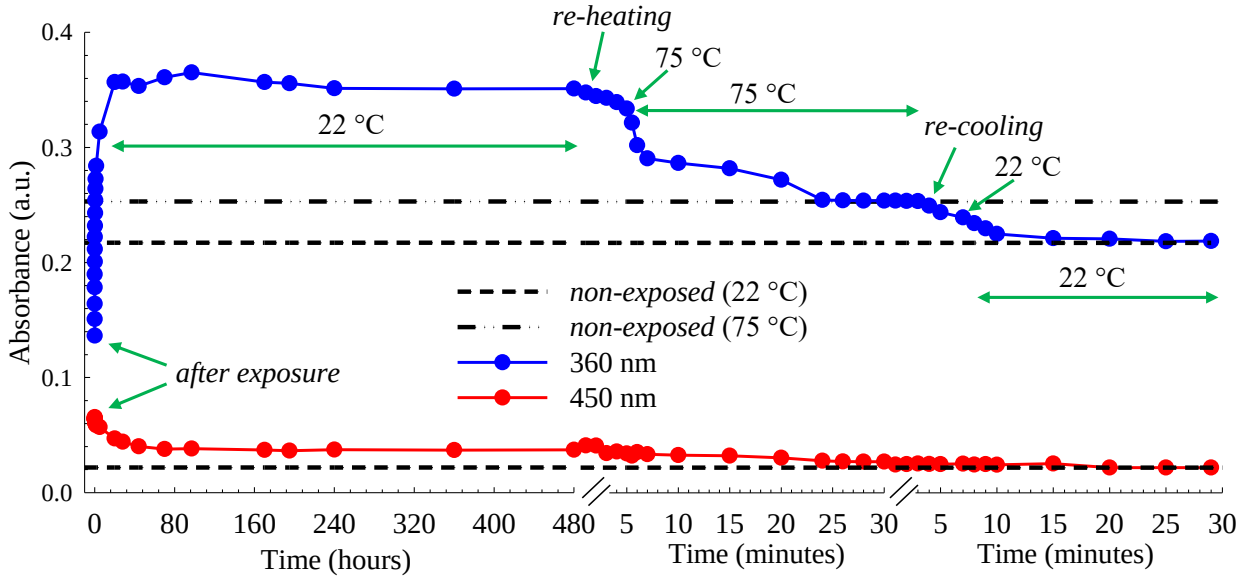

Figure 8. Absorbance recovery to the original non-exposed sample for the *trans* (360 nm) and *cis* (450 nm) isomers of MeOAzB-T film cast on a quartz substrate. The behavior reflects the ability to maintain the aggregate state for a long time after exposure and to control the recovery process by heating then cooling. See text for details.

CONCLUSIONS

In this work, we studied a new liquid crystalline terpolymer (MeOAzB-T) capable of trapping the absorbed photon energy upon exposure to UV light through *trans* → *cis* isomerization and molecular aggregation. Normal *trans* ← *cis* recovery was observed in solution (THF) after UV exposure, whereas the absorbance of the *trans* isomer exceeds the non-exposed level in glass and smectic phase. Full recovery took 365 hr in the glass state and 5 hr in the smectic phase. When the smectic phase (75 °C) was cooled down to the glassy state (22 °C) while keeping UV exposure, the absorbance of the *trans* isomer was maintained in the dark at a level higher than that of the non-exposed level, in a clear indication of transforming to a new, stable state (monitored for 20 days). The recovery process was unlocked when the sample was heated to 75 °C, then cooled to 22 °C, in which a full recovery was achieved.

In order to unravel the mechanism behind this unusual behavior, we tested the homopolymer analogue and replaced the methoxy group by NO_2/H. When comparing the absorption spectra of these compounds with that of MeOAzB-T, the new state of the polymer was assigned to H- and J-aggregation of the MeOAzB units. The spectral location of the two aggregates, with respect to the non-aggregated monomers, was qualitatively predicted by TD-DFT calculations. Femtosecond transient absorption spectroscopy at λ_{probe} = 400-420 nm revealed the ultrafast dynamics in the excited state of MeOAzB-T in THF solution, glass, and smectic phases. The first two dynamical processes were assigned to S_2 ($\pi\pi^*$) → S_1 ($n\pi^*$) vibrational relaxation and internal conversion (~ 100 fs), followed by *trans* ← *cis* isomerization and excited-state relaxation through S_1/S_0 conical intersection (1.5-3 ps). On the other hand, the final ground state recovery was measured to be 5.4 ps in THF solution, albeit much longer in glass (62 ps) and smectic phase (27 ps). The difference in the last decay component was correlated to more restricted motion in thin film, compared to solution. A long decay component was observed in the glass state (215 ps) and smectic phase (97 ps) when detecting at λ_{probe} = 550 nm and assigned to a long-lived intermediate state due to aggregation of the terpolymer. The stability of the excited state leads to more aggregation due to the larger dipole moment, compared to ground state that was observed in the TD-DFT calculations as an increase in the electron density at the central azo bond in the excited state. This may explain the absorbance increase of the *trans* isomer upon UV exposure.

Our results show the suitability of MeOAzB-T to act as a solar-thermal fuel in which the absorbed energy can be maintained for a long time at room temperature before it could be released by heating above the glass transition. Testing the ability of MeOAzB-T to store solar energy will be useful for practical uses such as absorbing sunlight and releasing it on demand.

Supporting Information. Absorption spectra and absorbance recovery for the HAzB-T film after irradiation, frontier molecular orbital plots for the H- and J-type aggregates of MeOAzB-T, kinetic traces at different probe wavelengths for MeOAzB-T, dielectric permittivity spectra for the MeOAzB-T film.

ACKNOWLEDGMENTS

OKAZ, JH, and ARI would like to acknowledge the Sultan Qaboos University for its support through His Majesty's Trust Fund for Strategic Research (SR/SCI/CHEM/18/01) and Internal Grant (IG/SCI/CHEM/21/03). SMA and NFKA would like to acknowledge Malaysian Ministry of Higher Education for the grant number 600-IRMI/FRGS 5/3 (374/2019). AMF would like to acknowledge the Carnegie Trust for the Universities of Scotland, for the Research Incentive Grant RIG008586, the Royal

Society and Specac Ltd., for the Research Grant RGS\R1\201397, the Royal Society of Chemistry for the award of a mobility grant (M19-0000), and the Royal Society of Edinburgh and the Scottish Government, for the award of a SAPHIRE project.

REFERENCES

1. Dong, L.; Feng, Y.; Wang, L.; Feng, W. Azobenzene-Based Solar Thermal Fuels: Design, Properties, and Applications. *Chem. Soc. Rev.* **2018,** *47*, 7339–7368.
2. Bléger, D.; Hecht, S. Visible-Light-Activated Molecular Switches. *Angew. Chem. Int.* **2015,** *54*, 11338–11349.
3. Matsuda, K.; Irie, M. Diarylethene as a Photoswitching Unit. *J. Photochem. Photobiol. C* **2004,** *5*, 169–182.
4. Hadjoudis, E.; Mavridis, I. M. Photochromism and Thermochromism of Schiff Bases in the Solid State: Structural Aspects. *Chem. Soc. Rev.* **2004,** *33*, 579–588.
5. van der Molen, S. J.; Liljeroth, P. Charge Transport Through Molecular Switches. *J. Phys.: Condens. Matter* **2010,** *22*, 133001.
6. Bubnov, A.; Cigl, M.; Sedláčková, N.; Pociecha, D.; Böhmová, Z.; Hamplová, V. Self-Assembling Behaviour of New Functional Photosensitive Cinnamoyl-Based Reactive Mesogens. *Liq. Cryst.* **2020,** *47*, 2276–2291.
7. Hartley, G. S. The Cis-Form of Azobenzene. *Nature* **1937,** *140*, 281–281.
8. Gelebart, A. H.; Mulder, D. J.; Varga, M.; Konya, A.; Vantomme, G.; Meijer, E. W.; Broer, D. J. Making Waves in a Photoactive Polymer Film. *Nature* **2017,** *546*, 632–636.
9. de Haan, L. T.; Gimenez-Pinto, V.; Konya, A.; Nguyen, T. S.; Verjans, J. M.; Sánchez-Somolinos, C.; Schenning, A. P. Accordion-Like Actuators of Multiple 3D Patterned Liquid Crystal Polymer Films. *Adv. Funct. Mater.* **2014,** *24*, 1251–1258.
10. Ichimura, K. Photoalignment of Liquid-Crystal Systems. *Chemical reviews*, **2000,** *100*, 1847-1874.
11. Paterson, D. A.; Xiang, J.; Singh, G.; Walker, R.; Agra-Kooijman, D. M.; Martínez-Felipe, A.; Imrie, C. T. Reversible Isothermal Twist–Bend Nematic–Nematic Phase Transition Driven by the Photoisomerization of an Azobenzene-Based Nonsymmetric Liquid Crystal Dimer. *J. Am. Chem. Soc.* **2016,** *138*(16), 5283–5289.
12. Chaganava, I.; Kilosanidze, B.; Kakauridze, G.; Oriol, L.; Piñol, M.; Martinez-Felipe, A. Induction of the Vector Polyphotochromism in Side-Chain Azopolymers. *J. Photochem. Photobiol. A* **2018,** *354*, 70–77.
13. Bobrovsky, A.; Mochalov, K.; Solovyeva, D.; Shibaev, V.; Cigl, M.; Hamplová, V.; Bubnov, A. Laser-Induced Formation of "Craters" and "Hills" in Azobenzene-Containing Polymethacrylate Films. *Soft Matter* **2020,** *16*, 5398–5405.
14. Bobrovsky, A.; Shibaev, V.; Cigl, M.; Hamplová, V.; Pociecha, D.; Bubnov, A. Azobenzene-Containing LC Polymethacrylates Highly Photosensitive in Broad Spectral Range. *J. Polym. Sci. A* **2016,** *54*, 2962–2970.
15. Bobrovsky, A.; Shibaev, V.; Piryazev, A.; Anokhin, D. V.; Ivanov, D. A.; Sinitsyna, O.; Bubnov, A. Photo-Orientation Phenomena in Photochromic Liquid Crystalline Azobenzene-Containing Polymethacrylates with Different Spacer Length. *Macromol. Chem. Phys.* **2017,** *218*, 1700127.
16. Bobrovsky, A.; Shibaev, V.; Cigl, M.; Hamplová, V.; Dorovatovskii, P.; Ostrovskii, B.; Bubnov, A. The Effect of Spacer and Alkyl Tail Lengths on the Photoorientation Processes in Amorphousized Films of Azobenzene-Containing Liquid Crystalline Polymethacrylates. *Liq. Cryst.* **2020,** *47*, 377–383.

17. Concellón, A.; Blasco, E.; Martínez-Felipe, A.; Martínez, J. C.; Šics, I.; Ezquerra, T. A.; Oriol, L. Light-Responsive Self-Assembled Materials by Supramolecular Post-Functionalization via Hydrogen Bonding of Amphiphilic Block Copolymers. *Macromol.* **2016,** *49*, 7825–7836.
18. Martinez-Felipe, A.; Brebner, F.; Zaton, D.; Concellon, A.; Ahmadi, S.; Piñol, M.; Oriol, L. Molecular Recognition via Hydrogen Bonding in Supramolecular Complexes: A Fourier Transform Infrared Spectroscopy Study. *Molecules* **2018,** *23*, 2278.
19. Kucharski, T. J.; Ferralis, N.; Kolpak, A. M.; Zheng, J. O.; Nocera, D. G.; Grossman, J. C. Templated Assembly of Photoswitches Significantly Increases the Energy-Storage Capacity of Solar Thermal Fuels. *Nat. chem.* **2014,** *6*, 441–447.
20. Feng, W.; Luo, W.; Feng, Y. Photo-Responsive Carbon Nanomaterials Functionalized by Azobenzene Moieties: Structures, Properties and Application. *Nanoscale* **2012,** *4*, 6118–6134.
21. Saydjari, A. K.; Weis, P.; Wu, S. Spanning the Solar Spectrum: Azopolymer Solar Thermal Fuels for Simultaneous UV and Visible Light Storage. *Adv. Energy Mater.* **2017,** *7*, 1601622.
22. Bandara, H. D.; Burdette, S. C. Photoisomerization in Different Classes of Azobenzene. *Chem. Soc. Rev.* **2012,** *41*, 1809–1825.
23. Vanti, L.; Alauddin, S. M.; Zaton, D.; Aripin, N. F. K.; Giacinti-Baschetti, M.; Imrie, C. T.; Martinez-Felipe, A. Ionically Conducting and Photoresponsive Liquid Crystalline Terpolymers: Towards Multifunctional Polymer Electrolytes. *Eur. Polym. J.* **2018,** *109*, 124–132.
24. Martinez-Felipe, A.; Lu, Z.; Henderson, P. A.; Picken, S. J.; Norder, B.; Imrie, C. T.; Ribes-Greus, A. Synthesis and Characterisation of Side Chain Liquid Crystal Copolymers Containing Sulfonic acid groups. *Polymer* **2012,** *53*, 2604–2612.
25. Alauddin, S. M.; Aripin, N. F. K.; Velayutham, T. S.; Chaganava, I.; Martinez-Felipe, A. The Role of Conductivity and Molecular Mobility on The Photoanisotropic Response of a New azo-polymer Containing Sulfonic Groups. *J. Photochem. Photobiol. A* **2020,** *389*, 112268.
26. Alauddin, S. M.; Aripin, N. F. K.; Velayutham, T. S.; Martinez-Felipe, A. Liquid Crystalline Copolymers Containing Sulfonic and Light-Responsive Groups: From Molecular Design to Conductivity. *Molecules* **2020,** *25*, 2579.
27. Martínez-Felipe, A. Liquid Crystal Polymers and Ionomers for Membrane Applications. *Liq. Cryst.* **2011,** *38*, 1607–1626.
28. Alauddin, S. M.; Ibrahim, A. R.; Aripin, N. F. K.; Velayutham, T. S.; Abou-Zied, O. K.; Martinez-Felipe, A. New Side-Chain Liquid Crystalline Terpolymers with Anhydrous Conductivity: Effect of Azobenzene Substitution on Light Response and Charge Transfer. *Eur. Polym. J.* **2021,** *146*, 110246.
29. Liang, T.; van Kuringen, H. P.; Mulder, D. J.; Tan, S.; Wu, Y.; Borneman, Z.; Schenning, A. P. Anisotropic Dye Adsorption and Anhydrous Proton Conductivity in Smectic Liquid Crystal Networks: The Role of Cross-Link Density, Order, and Orientation. *ACS Appl. Mater. Interfaces* **2017,** *9*, 35218–35225.
30. Yang, X.; Tan, S.; Liang, T.; Wei, B.; Wu, Y. A Unidomain Membrane Prepared from Liquid-Crystalline Poly (Pyridinium 4-Styrene Sulfonate) for Anhydrous Proton Conduction. *J. Membr. Sci.* **2017,** *523*, 355–360.
31. Kobayashi, T.; Ichikawa, T.; Kato, T.; Ohno, H. Development of Glassy Bicontinuous Cubic Liquid Crystals for Solid Proton-Conductive Materials. *Adv. Mater.* **2017,** *29*, 1604429.
32. Concellón, A.; Liang, T.; Schenning, A. P.; Serrano, J. L.; Romero, P.; Marcos, M. Proton-Conductive Materials Formed by Coumarin Photocrosslinked Ionic Liquid Crystal Dendrimers. *J. Mater. Chem. C* **2018,** *6*, 1000–1007.

33. Gong, M.; Song, F.; Li, H.; Lin, X.; Wang, J.; Zhang, L.; Wang, D. Optimizing Energy Harvesting Performance of Silicone Elastomers by Molecular Grafting of Azobenzene to the Macromolecular Network. *RSC Adv.* **2021,** *11,* 19088−19094.
34. Cook, A. G.; Inkster, R. T.; Martinez-Felipe, A.; Ribes-Greus, A.; Hamley, I. W.; Imrie, C. T. Synthesis and Phase Behaviour of a Homologous Series of Polymethacrylate-Based Side-Chain Liquid Crystal Polymers. *Eur. Polym. J.* **2012,** *48*, 821–829.
35. Ibrahim, I.; Lim, H. N.; Abou-Zied, O. K.; Huang, N. M.; Estrela, P.; Pandikumar, A. Cadmium Sulfide Nanoparticles Decorated with Au Quantum Dots as Ultrasensitive Photoelectrochemical Sensor for Selective Detection of Copper(II) Ions. *J. Phys. Chem. C* **2016,** 120, 22202–22214.
36. Kumar, G. S.; Neckers, D. C. Photochemistry of Azobenzene-Containing Polymers. *Chem. Rev.* **1989**, *89*, 1915–1925.
37. Gagliardi, L.; Orlandi, G.; Bernardi, F.; Cembran, A.; Garavelli, M. A Theoretical Study of the Lowest Electronic States of Azobenzene: The Role of Torsion Coordinate in the cis−trans Photoisomerization. *Theor. Chem. Acc.* **2004**, *111*, 363–372.
38. Zhao, Y.; Ikeda, T. (Editors), Smart Light-Responsive Materials: Azobenzene-Containing Polymers and Liquid Crystals, Wiley: New Jersey 2009.
39. Fujino, T.; Tahara, T. Picosecond Time-Resolved Raman Study oftrans-Azobenzene. *J. Phys. Chem. A* **2000**, *104*, 4203–4210.
40. Pedersen, T. G.; Johansen, P. M.; Holme, N. C. R.; Ramanujam, P. S.; Hvilsted, S. Mean Field Theory of Photoinduced Formation of Surface Reliefs in Side Chain Azobenzene Polymers. *Phys. Rev. Lett.* **1998**, *80*, 89–92.
41. Frisch, M. J.; Trucks, G. W.; Schlegel, H. B.; Scuseria, G. E.; Robb, M. A.; Cheeseman, J. R.; Scalmani, G.; Barone, V.; Mennucci, B.; Petersson, G. A., et al. *Gaussian 09*, Revision E.1; Gaussian, Inc.: Wallingford, CT, 2013.
42. Aleotti, F.;Nenov, A.; Salvigni, L.; Bonfanti, M.; El-Tahawy, M. M.; Giunchi, A.; Gentile, M.; Spallacci, C.; Ventimiglia, A.; Cirillo, G., et al. Spectral Tuning and Photoisomerization Efficiency in Push−Pull Azobenzenes: Designing Principles. *J. Phys. Chem. A* **2020**, *124*, 9513−9523.
43. Andersson, J.-Å; Petterson, R.; Tegnér, L. Flash Photolysis Experiments in the Vapour Phase at Elevated Temperatures I: Spectra of Azobenzene and the Kinetics of Its Thermal cis-trans Isomerization. *J. Photochem.* **1982**, *20*, 17–32.
44. Tang, Z.; Johal, M. S.; Scudder, P.; Caculitan, N.; Magyar, R. J.; Tretiak, S.; Wang, H.-L. Study of the Non-Covalent Interactions in Langmuir–Blodgett Films: An Interplay Between π–π and Dipole–Dipole Interactions. *Thin Solid Films* **2007**, *516*, 58–66.
45. Monti, S.; Orlandi, G.; Palmieri, P. Features of the Photochemically Active State Surfaces of Azobenzene. *Chem. Phys.* **1982**, *71*, 87–99.
46. Cattaneo, P.; Persico, M. An *Ab initio* Study of the Photochemistry of Azobenzene. *Phys. Chem. Chem. Phys.* **1999**, *1*, 4739–4743.
47. Rau, H. Photochromism: Molecules and Systems; Elsevier: Amsterdam, 1990; Chapter 4.
48. Azuma, J.; Tamai, N.; Shishido, A.; Ikeda, T. Femtosecond Dynamics and Stimulated Emission from the S_2 State of a Liquid Crystalline *trans*-Azobenzene. *Chem. Phys. Lett.* **1998**, *288*, 77–82.
49. Mayer, S. G.; Thomsen, C. L.; Philpott, M. P.; Reid, P. J. The Solvent-Dependent Isomerization Dynamics of 4-(Dimethylamino)azobenzene (DMAAB) Studied by Subpicosecond Pump–Probe Spectroscopy. *Chem. Phys. Lett.* **1999**, *314*, 246–254.
50. Tamai, N.; Miyasaka, H. Ultrafast Dynamics of Photochromic Systems. *Chem. Rev.* **2000**, *100*, 1875−1890.

51. Hirose, Y.; Yui, H.; Sawada, T. Effect of Potential Energy Gap between the *n*-π^* and the π-π^* State on Ultrafast Photoisomerization Dynamics of an Azobenzene Derivative. *J. Phys. Chem. A* **2002,** *106*, 3067−3071.
52. Chang, C.–W.; Lu, Y.-C.; Wang, T.T.; Diau, E. W.G. Photoisomerization Dynamics of Azobenzene in Solution with S_1 Excitation: A Femtosecond Fluorescence Anisotropy Study. *J. Am. Chem. Soc*. **2004**, *126*, 10109-10118
53. Quick, M.; Dobryakov, A. L.; Gerecke, M.; Richter, C.; Berndt, F.; Ioffe, I. N.; Granovsky, A. A.; Mahrwald, R.; Ernsting, N. P.; Kovalenko, S. A. Photoisomerization Dynamics and Pathways of Trans- and Cis-Azobenzene in Solution from Broadband Femtosecond Spectroscopies and Calculations. *J. Phys. Chem. B* **2014**, *118*, 8756–8771.
54. Nenov, A.; Borrego-Varillas, R.; Oriana, A.; Ganzer, L.; Segatta, F.; Conti, I.; Segarra-Marti, J.; Omachi, J.; Dapor, M.; Taioli, S., et al. UV-Light-Induced Vibrational Coherences: The Key to Understand Kasha Rule Violation in *trans*-Azobenzene. *J. Phys. Chem. Lett.* **2018**, *9*, 1534–1541.
55. Otolski, C. J.; Raj, A. M.; Ramamurthy, V.; Elles, C. G. Ultrafast Dynamics of Encapsulated Molecules Reveals New Insight on the Photoisomerization Mechanism for Azobenzenes. *J. Phys. Chem. Lett.* **2019**, *10*, 121–127.
56. Fujino, T.; Arzhantsev, S. Y.; Tahara, T. Femtosecond Time-Resolved Fluorescence Study of Photoisomerization of *trans*-Azobenzene. *J. Phys. Chem. A* **2001**, *105*, 8123–8129.
57. Lednev, I. K.; Ye, T. Q.; Hester, R. E.; Moore, J. N. Femtosecond Time-Resolved UV-Visible Absorption Spectroscopy of *trans*-Azobenzene in Solution. *J. Phys. Chem.* **1996**, *100*, 13338–13341.
58. Satzger, H.; Root, C.; Braun, M. Excited-State Dynamics of *trans*- and *cis*-Azobenzene after UV Excitation in the $\pi\pi^*$ Band. *J. Phys. Chem. A* **2004**, *108*, 6265–6271.
59. Lednev, I. K.; Ye, T.-Q.; Matousek, P.; Towrie, M.; Foggi, P.; Neuwahl, F. V. R.; Umapathy, S.; Hester, R. E.; Moore, J. N. Femtosecond Time-Resolved UV-Visible Absorption Spectroscopy of *trans*-azobenzene: Dependence on Excitation Wavelength. *Chem. Phys. Lett.* **1998**, *290*, 68–74.
60. Bahrenburg, J.; Renth, F.; Temps, F.; Plamper, F.; Richtering, W. Femtosecond Spectroscopy Reveals Huge Differences in the Photoisomerisation Dynamics between Azobenzenes Linked to Polymers and Azobenzenes in Solution. *Phys. Chem. Chem. Phys.* **2014**, *16*, 11549−11554.
61. Schmidt, B.; Sobotta, C.; Malkmus, S.; Laimgruber, S.; Braun, M.; Zinth, W.; Gilch, P. Femtosecond Fluorescence and Absorption Dynamics of an Azobenzene with a Strong Push-Pull Substitution. *J. Phys. Chem. A* **2004**, *108*, 4399−4404.

TOC Graphic

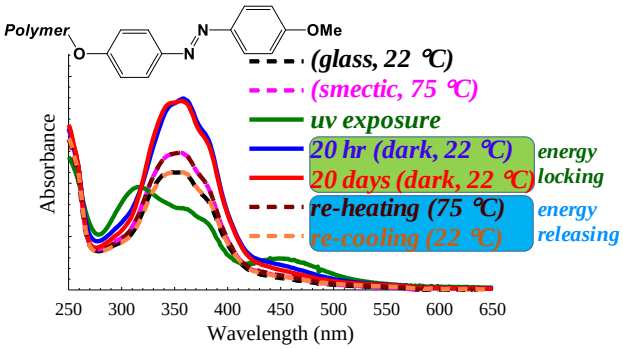
Polymer
O
N
N
OMe
(glass, 22 ℃)
(smectic, 75 ℃)
uv exposure
20 hr (dark, 22 ℃)
20 days (dark, 22 ℃)
re-heating (75 ℃)
re-cooling (22 ℃)
energy locking
energy releasing
Absorbance
250 300 350 400 450 500 550 600 650
Wavelength (nm)